Assessing the potential of drone-based thermal infrared imagery for quantifying river temperature heterogeneity

Stephen J Dugdale[1,*,†], Christa A Kelleher[2], Iain A Malcolm[3], Samuel Caldwell[2], David M Hannah[1]

[1]School of Geography, Earth and Environmental Sciences, University of Birmingham, Edgbaston, Birmingham, B15 2TT, UK
[2]Earth Sciences, Syracuse University, Syracuse, New York, 13244, USA
[3]Marine Scotland Science, Freshwater Fisheries Laboratory, Faskally, Pitlochry, PH16 5LB, UK

*Correspondence to: stephen.dugdale@nottingham.ac.uk
[†]Now at: School of Geography, University of Nottingham, University Park, Nottingham, NG7 2RD, UK

Running title: Drone thermal imaging of river temperature

Keywords: unoccupied aerial systems, drones, thermal infrared, TIR, river temperature, temperature heterogeneity, climate change, remote sensing

5509 words

Abstract

Climate change is altering river temperature regimes, modifying the dynamics of temperature-sensitive fishes. The ability to map river temperature is therefore important for understanding the impacts of future warming. Thermal infrared (TIR) remote sensing has proven effective for river temperature mapping, but TIR surveys of rivers remain expensive. Recent drone-based TIR systems present a potential solution to this problem. However, information regarding the utility of these miniaturised systems for surveying rivers is limited. Here, we present the results of several drone-based TIR surveys conducted with a view to understanding their suitability for characterising river temperature heterogeneity. We find that drone-based TIR data is able to clearly reveal the location and extent of discrete thermal inputs to rivers, but thermal imagery suffers from temperature drift-induced bias which prevents the extraction of accurate temperature data. Statistical analysis of the causes of this drift reveals that drone flight characteristics and environmental conditions at the time of acquisition explain ~66% of the variance in TIR sensor drift. These results shed important light on the factors influencing drone-based TIR data quality, and suggest that further technological development is required to enable the extraction of robust river temperature data. Nonetheless, this technology represents a promising approach for augmenting *in-situ* sensor capabilities and improved quantification of advective inputs to rivers at intermediate spatial scales between point measurements and 'conventional' airborne or satellite remote sensing.

1. Introduction

Rivers exhibit mosaics of warm and cool water habitat, which are highly variable through space and time (Fullerton et al. 2018; Steel et al. 2017; Torgersen et al. 2001). Because water temperature influences physico-chemical processes and biological activity in rivers (Caissie 2006; Webb et al. 2008), this heterogeneity exerts considerable influence on the distribution, behaviour and abundance of numerous cold water-adapted fish species (e.g., Brewitt and Danner 2014; Isaak et al. 2015; Tonolla et al. 2012). River temperature regimes are changing, with both climate warming and cooling trends reported (Arismendi et al. 2012; Chen et al. 2016; Hannah and Garner 2015). Despite increasing research, there remains considerable uncertainty regarding the response of specific river ecosystems to future climate change (Garner et al. 2017a) given complex interactions between climate, hydrology and human activity (Arnell and Gosling 2013; Jones et al. 2012; Kurylyk et al. 2015a; Taylor et al. 2012). There is therefore an urgent need to quantify river temperature heterogeneity to improve understanding of the nature and impacts of drivers of change on river systems.

High resolution thermal infrared (TIR) remote sensing has been widely used to map river temperature variability (see Dugdale 2016 for review). Investigations using TIR have revealed the presence of temperature heterogeneity at two distinct spatial scales (termed *diffuse* and *discrete* herein; Dugdale 2016). Diffuse heterogeneity manifests as gradual warming or cooling of river temperature over streamwise scales of 10^2 – 10^4 m. These longitudinal temperature trends are caused typically by spatial variability in energy fluxes (related to changes in altitude/topography), channel hydraulics and non-point source hydrological exchanges often linked to river basin properties (e.g., land-use, geology; Eschbach et al. 2017; Garner et al. 2017b; Wawrzyniak et al. 2016). Diffuse temperature heterogeneity does not necessarily imply a downstream warming trend (see Fullerton et al. 2015), but rather refers to gradual warming *and* cooling patterns contained within a river's longitudinal temperature profile. Conversely, discrete heterogeneity refers to localised temperature changes caused by advective contributions from tributaries, localised groundwater upwelling (Dugdale et al. 2013) or other point sources. Heterogeneity at this scale can involve both 'abrupt' changes in temperature related to isolated advective inputs at the scale of 10^0 m (such as tributaries), but

can also refer to inputs such as groundwater seepage which cause a less immediate change in temperature, but occur over larger distances (eg. 10^1). These discrete inputs of cool or warm water often play a crucial role in the provision of thermal refuges (Daigle et al. 2015; Ebersole et al. 2015; Kurylyk et al. 2015b). Despite the wealth of river temperature data that TIR has generated (Dugdale et al. 2015; Fullerton et al. 2015; Tan and Cherkauer 2013) and its role in improving process-based understanding of river temperature heterogeneity, TIR surveys of river corridors remain relatively costly, making it difficult to justify their use along shorter reaches or for multi-temporal surveys (Lee et al. 2016).

Recent advances in small Unoccupied Aerial Systems (sUAS), commonly known as drones, provide a potential solution to this problem. sUAS are relatively inexpensive to obtain and deploy. Their versatility means that they can be used to rapidly image remote locations (e.g., 1 km in ≥ 15 min), and their ease of use enables multiple repeatable surveys. Thus, sUAS equipped with thermal infrared cameras have the potential to revolutionize the collection of river temperature data. While early examples of UAS-based TIR (e.g., Jensen et al. 2012; Lee et al. 2016; Wawrzyniak et al. 2013) used conventional 'handheld' thermal imaging cameras mounted to larger drones, advances in TIR sensor miniaturisation have heralded a new generation of compact TIR cameras that are integrated fully with sUAS. However, the only articles in the peer-reviewed literature demonstrating the use of these miniaturised systems in the river sciences (Abolt et al., 2018; Briggs et al, 2018) focus on their use for monitoring groundwater-surface water exchange. No study has formally assessed the performance of these solutions for monitoring river temperature heterogeneity, particularly at spatial scales amenable to the enhanced understanding and management of river temperature regimes. In this context, this article evaluates the utility of an off-the-shelf lightweight integrated sUAS/TIR package for mapping river temperature heterogeneity. We report proof-of-concept results of sUAS-based TIR surveys conducted in two hydromorphologically and geologically distinct watersheds known to contain diffuse thermal heterogeneity (Baddoch Burn, Scotland, UK) and discrete temperature inputs (Onondaga Creek, New York, USA). Our specific objectives were: (1) to characterise diffuse and discrete river temperature heterogeneity from sUAS-based TIR data, (2) to compare sUAS-derived river temperature data to observations from in-stream temperature records and (3) to understand sources of bias in sUAS-based TIR data and discuss limitations/solutions.

2. Methodology

2.1 Study sites

2.2.1 Baddoch Burn, Scotland

The Baddoch Burn is a tributary of the Aberdeenshire River Dee, Scotland where Marine Scotland have monitored salmon populations since 1988 (Figure 1a). The catchment drains an area of ~23.0 km^2. Mean annual discharge is ~0.92 $m^3 s^{-1}$; seasonal patterns of precipitation and snowmelt lead to lower flows during the summer months and increased discharge between autumn and spring. Land-use is predominantly open heather moorland. During summer of 2017, repeat thermal infrared imagery was obtained from a ~1.2km stretch of river to assess the ability of sUAS-based TIR to characterise diffuse stream temperature heterogeneity. The study stretch is a semi-confined channel (bankfull width ~10 m) with a relatively shallow gradient and wide floodplain.

2.1.2. Onondaga Creek, NY, USA

Onondaga Creek drains a catchment of 231 km^2 in Syracuse, NY, USA (Figure 1b). Mean annual discharge is approximately 5.59 $m^3 s^{-1}$, with streamflow peaks in winter or spring in response to cycles of snowmelt and precipitation, and low streamflow through summer and fall. Study imagery in May and July of 2017 was collected along two reaches to assess the utility of sUAS-based TIR for quantifying discrete thermal inputs to streams. The first reach (bankfull width ~27 m; 170 m long) ends at a concrete spillway and contains a natural spring. The second reach (bankfull width ~15 m; 275 m long) includes inflow from an active stormwater culvert.

2.2 Thermal image acquisition and processing

2.2.1 Baddoch Burn, Scotland

Thermal imagery of the Baddoch Burn was acquired on 10 occasions over three days in May and June 2017. We used a DJI Inspire 1 quadcopter equipped with a DJI Zenmuse XT Radiometric thermal imaging camera (336 x 256 pixels, 7.5-13.5 µm; based on the FLIR Tau 2 camera core). Flights were conducted between 11:00 and 18:00 to capture the evolution in longitudinal temperature heterogeneity as the river warmed through the morning and early afternoon until its thermal maximum (generally between 16:00 and 17:00). Further details of each flight are given in Table 1. ExifTool (Harvey 2018) was used to convert raw data to radiant temperature (T_R) using Planck's radiation law and flight altitude, air temperature and relative humidity as inputs. The resulting images were individually orthorectified using Agisoft Photoscan Professional (Agisoft 2017). A custom MATLAB (MathWorks, 2016) script was applied to the TIR orthophotos to extract a temperature long profile for each of the 10 surveys by computing the mean temperature from a 5 m buffer at regularly intervals (2.5 m) along the river's centreline. Temperature jumps resulting from the camera's non-uniformity correction system were removed (as suggested by Dugdale, 2016). Finally, long profiles were filtered using a 10 m moving average to remove minor noise caused by non-water objects (i.e. bridges, exposed river gravel).

2.2.2 Onondaga Creek, NY

Thermal images were collected in Syracuse, NY, on 12 May and 19 July 2017 using an identical sUAS model and camera as used in Baddoch Burn. Flight characteristics were held constant for Syracuse flights (see Table 2). Another application of TIR videography at this location from data collected in June 2017 can be found in Fitch et al. (2018). Images were post-corrected based on local air temperature, relative humidity, flight altitude and reflective temperature using FLIR Tools (FLIR 2018). Images were then georeferenced in ArcGIS. Radiant temperatures (T_R) were determined from raw georeferenced TIR imagery and reported as a mean and standard deviation within the spring plume and within a 5 m buffer of the stream centreline. Apparent stream temperature gradients within each image resulting from solar and skylight reflections made the visual discrimination of discrete thermal inputs difficult from the raw image mosaics. Therefore, image digital number (DN) values were adjusted manually in Adobe Photoshop (Adobe 2017) to minimize temperature offsets between collocated images resulting from drift and solar reflections. This produced an adjusted TIR dataset that precluded quantitative extraction of stream temperatures but more clearly permitted delineation of thermal plumes resulting from discrete advective inputs.

2.3 Evaluation of TIR-derived river temperature heterogeneity

2.3.1 Diffuse temperature heterogeneity (Baddoch Burn)

Kinetic (ie. in-stream) temperature data (T_K) in the Baddoch Burn was recorded at 15 min intervals by three TinyTag Aquatic 2 loggers (cross-calibrated to give accuracy ±0.02 °C) and two Campbell Scientific 107 temperature probes (accuracy ±0.2 °C) attached to two automated weather stations (AWSs). For each of the 10 surveys, we compared temperatures recorded by the loggers to radiant temperatures extracted from corresponding locations in the TIR-derived long profiles. Prior to this comparison, it was necessary to remove systematic bias in the TIR data resulting from atmospheric distortion (eg. Dugdale 2016 and Handcock et al. 2006). This can either be achieved through modifying the TIR image transmissivity values, or more simply through the addition/subtraction of a constant offset value (ie. correction factor). Here, we applied a correction factor to each long profile to minimise the mean difference (bias) between TIR and corresponding kinetic temperature observations, thus removing the systematic atmospheric bias. The ability of sUAS-based TIR to characterise diffuse temperature variability was subsequently evaluated by computing the root mean squared error (RMSE) and R^2 between observations of T_K and T_R. We also compared the mean and standard deviation of each (entire) T_R long profile against that of the T_K loggers.

All non-cooled microbolometer TIR cameras (such as the FLIR Tau 2) are susceptible to temperature drift (ie. non-monotic temperature bias between successive images correlated to camera operation time). This is generally caused by external radiative warming of the camera case and internal heating of the TIR sensor (Olbrycht et al. 2012; Strąkowki 2017; Wolf et al. 2016), but is typically automatically compensated by hardware and software on the sensor (eg. the inclusion of a thermistor to measure and thus correct for the temperature of the sensor's electronics; Abolt et al. 2018). Preliminary analyses of data collected during the Baddoch Burn surveys indicated a substantially higher magnitude of drift than that reported by other studies employing non-cooled cameras (eg. Dugdale et al. 2013; Rautio et al. 2015; Wawrzyniak et al. 2016). To identify the potential drivers of this drift in our TIR imagery (and hence, inform potential avoidance strategies), we extracted metrics describing the sUAS flight characteristics and environmental conditions during each survey that could potentially influence this measurement error (see Supporting Information Table S1). These comprised sine and cosine of TIR camera yaw (sin_{cam}, cos_{cam}), sine and cosine of stream azimuth (sin_{azm}, cos_{azm}), altitude (*alt*), seconds elapsed since midnight (*time*) and meteorological conditions (air temperature (T_a), humidity (*RH*) incoming solar shortwave radiation (K_{in}) and net longwave radiation (Q^*) derived from the AWSs) at time of image capture. We also applied the 'Area Solar Radiation' tool in ArcGIS (ESRI, 2014) to a 5m DEM of the study area to calculate the impact of topographic shading on solar radiation received above the stream. The resulting solar radiation raster (computed separately for each survey to account for the time/date of each drone flight) was subsequently sampled at discrete points along the stream centreline to give the streamwise variation in topographic shading (*TS*). All data were resampled at the resolution of the temperature long profiles using parametric cubic spline interpolation, and a random sample of 10% of these data retained for analysis to minimise spatial autocorrelation. K_{in} and Q^* were strongly collinear so Q^* was removed from the dataset; collinearity between the remaining metrics was minimal. We used stepwise multiple linear regression to identify links between the above metrics and temperature variability. Model selection was conducted by means of a step-up-down procedure using Bayesian Information Criterion (BIC) as model performance criterion. We started with an intercept-only model and subsequently added or removed predictors until BIC was no longer improved. The importance of each metric was assessed by removing it from the final model and computing the change in BIC (ie. the metric's ΔBIC value). We subsequently applied canonical correlation analysis (CCA) to the data to visualise the resulting multi-dimensional relationship between the various metrics and the temperature long profiles.

2.3.2 Discrete thermal inputs (Onondaga Creek)

Onondaga Creek stream temperature (T_K) was measured every 10 minutes with Thermochron iButton loggers (accuracy ±0.5°C, resolution 0.0625°C) secured within cavities just below the water surface on wooden stakes. Two stakes were installed within the main channel and two stakes were placed just before a 3 m long human-engineered rock channel that transmits spring water to the Creek (Figure 1b). Measurements of spring water temperature were made at this location to enable direct comparison to spring outflow, as the rock channel prohibited installation of any instrumentation nearer to the Creek confluence. The ability of sUAS-based TIR to quantify the temperature of discrete thermal inputs was assessed by comparing the mean temperature and temperature difference between in-stream observations from the loggers (T_K) and corresponding locations in the thermal images (T_R) for May and June 2017 flights.

3. Results

3.1 Characterisation of diffuse temperature heterogeneity (Baddoch Burn)

Visual inspection of the thermal image mosaics generated by the TIR surveys of Baddoch Burn (Figure 2) indicates that the Zenmuse XT Radiometric (FLIR Tau 2 based-) camera suffers from substantial temperature drift (ie. inter-image bias). Indeed, comparison of temperature long profiles derived from this data with in-stream records (figure 3) indicates that this drift results in an almost complete lack of association between the TIR-derived radiant temperature (T_R) and logger values (T_K; $R^2 = 0.01$, RMSE = 2.61 °C, n = 50) over 10 survey flights. Furthermore, the reach-averaged mean and standard deviation of computed from the TIR long profiles is markedly different to logger observations (see Supporting Information Table S2), meaning that even after the removal of global systematic bias (see 2.3.1) from the long profiles, considerable inter-image bias remains due to temperature drift.

Despite these results, the TIR long profiles reveal several key features. First, certain long profiles (e.g., flights 05 and 08) indicate a relatively low amount of drift within the streamwise confines of the loggers, with a standard deviation of < 1 °C. Second, several long profiles (e.g., flights 03 & 04, 05 & 08) display spatial (longitudinal) temperature patterns that persist across several surveys (ie. temperature peaks and troughs at broadly similar streamwise locations); this suggests that inter-image bias is spatio-temporally correlated and hence that TIR temperature drift may be the result of internal and external drivers. Indeed, the stepwise linear regression analysis (Table 3) and CCA (Figure 4) reveals that the temperature long profiles (and hence, magnitude of temperature drift) are significantly influenced by the flight characteristics and environmental metrics detailed in section 2.4. Results of these analyses indicate that the various metrics explained 66% of the variance in the temperature long profiles ($R^2 = 0.66$, $p < 0.001$; Table 3), with K_{in} being the most important (influential) covariate (ie. greatest ΔBIC), followed by *time, TS, RH* and T_a. The influence of sin_{cam}, *alt* and sin_{azm} were an order of magnitude smaller, albeit still significant, while cos_{cam} and cos_{azm} were not significant.

3.2 Quantification of discrete thermal inputs (Onondaga Creek)

TIR surveys of Onondaga Creek highlight the utility of sUAS-based TIR to quantify the temperature difference and extent of discrete thermal inputs (i.e. springs, culverts, and tributaries). While average differences between thermal plumes and channel temperatures were approximated closely by TIR imagery in May (T_K

difference of 0.7°C; T_R difference of 0.5°C; see Supporting Information Table S3), differences were poorly matched in July (T_K difference of 5.0°C; T_R difference of 2.1°C). The Syracuse data (and to a lesser extent, the Baddoch Burn dataset) also suffer from within-image biases due to solar and skylight reflections. This bias manifests as an apparent 'warming' gradient across each image frame, varying in magnitude but generating as much as 4 °C difference between the top and bottom of a single image, despite image acquisition at nadir. Even following manual adjustments, images displayed a streamwise thermal gradient (eg. cooling; Figure 5b; warming; Figure 5c). However, the existence of this gradient was not supported by stream temperature measurements taken during surveys, which indicate, at most, 1 °C warming across 2.2 km. Thus, similar manual adjustments to images may identify the impact of discrete inputs (e.g., springs or stormwater), but misrepresent general long profile trends.

Despite these challenges, TIR imagery clearly has potential for delineating the 2D surface extent of thermal plumes (Figure 5). Following appropriate manual correction for the effects of solar/skylight reflections, images of the spring (Figure 5a) and stormwater plumes (Figure 5b, c) can be applied to constrain the surface dimensions and seasonal variability of thermal plumes. In particular, while smaller differences between stormwater and channel temperatures produced a short plume in May (Figure 5b), increased temperature differences (ie. warmer channel vs cooler stormwater) yielded a more extensive plume in July (Figure 5c). However, it is nonetheless pertinent to note that the 2D surface manifestation of thermal plumes may differ substantially from their subsurface dimensions, especially during times of maximum temperature difference between the plume and main stem which will cause buoyancy differences and impact mixing.

4. Discussion

4.1 Challenges and opportunities for sUAS-Based TIR

sUAS-based TIR enables repeatable, low-altitude surveys at lower cost than 'conventional' (i.e. helicopter/aeroplane-based) airborne TIR (Lee et al., 2016) while producing high resolution images captured at nadir. Though these merits make sUAS-based TIR an attractive method for thermal imaging of waterbodies, susceptibility to within- and inter-image temperature biases presents an impediment to the extraction of true temperature data. Unlike 'conventional' airborne TIR which has repeatedly been shown to characterise stream temperature with a high degree of accuracy (ie. within 0.5 °C of T_K; Dugdale 2016; Handcock et al. 2012; Torgersen et al. 2001), we found that sUAS-based TIR poorly matched T_K observations at both sites. While empirical corrections using relationships between kinetic and radiant temperatures have been used to surmount these issues (e.g. Jensen et al. 2013), our findings suggest that this type of correction may not be capable of adequately compensating for non-monotonic drift which results from complex interactions between flight characteristics and environmental conditions that may change from site to site, from flight to flight, and even within a single flight. This is particularly evident from the Baddoch Burn surveys (Figures 2 and 3), which highlight the extent to which observed longitudinal temperature data are obscured by TIR drift. This drift renders the characterisation of true diffuse temperature heterogeneity extremely difficult with current sUAS-based TIR sensor technology. We also found that within-image biases resulting from solar/skylight reflections across images (Fig 3) may be especially pernicious in sUAS TIR data (compared to conventional TIR). This is potentially due to the use of a (relatively) wide angle lens, which is required when conducting flights at low altitude, reducing the angle of incidence between the sensor and water surface at locations towards the edge of the lens's field of view (eg. Kim et al. 2013). Increased within-image biases may also result from vignetting which is also associated with wider angle lenses (eg. Goldman, 2010; Kelcey and Lucieer, 2012). Although we acknowledge that only one type of TIR sensor was tested in the current study, many of the currently-available miniaturised TIR camera solutions are derivatives of this same sensor,

rendering our findings relevant to others using similar TIR cameras. Indeed, a recent study by Abolt et al. (2018) reported similar issues of temperature drift with both the FLIR Tau 2 sensor (upon which the DJI Zenmuse XT camera used in this study is based) and also the FLIR Vue Pro sensor, indicating that this problem is both a) relatively common and b) not limited to one particular camera model. Similarly, recent work with UAV-TIR imaging of glacier temperatures revealed temperature drift of a comparable magnitude using a SenseFly ThermoMap TIR camera, albeit under very different environmental conditions (Kraaijenbrink et al. 2018). During the current study we tested three versions of the same camera which all generated very similar results, emphasising that observed drift was not an artefact of a single faulty camera. Taken together, these results highlight the current challenges surrounding the derivation of diffuse temperature heterogeneity from sUAS. Although we acknowledge that there exist a other miniaturised TIR cameras which may not suffer from similar problems, we conclude that popular miniaturized TIR cameras based upon the TIR sensors/cores described above are more susceptible to drift than 'conventional' TIR systems. It is possible that greater drift results from insufficient insulation (or shielding) from external influences in comparison to larger TIR cameras. However, we also hypothesise that camera miniaturisation necessitates closer mounting of electronic components, potentially resulting in increased heat build-up (e.g., Ribeiro-Gomes et al. 2017; Kraaijenbrink et al. 2018) and thus greater temperature drift in comparison to larger TIR cameras. This presents a continued challenge for sUAS-based TIR imagery acquisition.

We were also surprised that TIR was unable to accurately quantify the difference between plume and main stem temperature during the July 2017 survey of Onondaga Creek (given this analysis was conducted using a single image and is hence unaffected by inter-image temperature drift). The poorer performance of TIR in July may result from differences in mixing of the cooler plume water between May and July, due to either changes in flow/velocity between the two surveys, or the increased temperature difference between the main stem and inflow (in comparison to May) which can cause the cool inflow to 'plunge' underneath the warmer main stem water mass due to its reduced buoyancy, thus complicating its measurement at the surface using TIR (eg. Handcock et al. 2006). Because TIR is only sensitive to surface values, substantial differences in mixing may have resulted in surface temperatures that are not representative of the true T_K value of the temperature inflow, and instead, reflect a combination of the both the main stem and plume temperature. Thus, season (both explicitly and implicitly) as well as temperature difference between the input and main channel may affect the ability of sUAS-based TIR to assess discrete temperature heterogeneity. Nevertheless, TIR surveys of Onondaga Creek highlight the capabilities of sUAS-based TIR imagery for delivering high-resolution 2D images that can be used to identify the location of discrete advective contributions, with the reduced sUAS flight altitude (and thus, increased image resolution) clear delineation of the plume's surface extent. By combining TIR data with spatially explicit in-situ measurements from logger grids of distributed temperature sensing (DTS) systems, drone-based TIR holds significant promise for quantifying the three-dimensional form of discrete advective inputs to river systems. The applications explored here include plumes resulting from natural springs and stormwater, demonstrating that sUAS-based TIR can be useful for detecting impacts of natural and human-derived sources. Other potential uses include assessment of thermal effluent from power plants (required under the US Clean Water Act and the EU Water Framework Direct; Miara et al. 2014) and dams. Alongside human impacts, there is also recent interest in TIR for mapping potential cool water refuges used by freshwater species to avoid heat stress (e.g. Frechette et al. 2018; George et al. 2016; Wawrzyniak et al. 2016); identifying these refuges is crucial in light of projected climate change. sUAS-based TIR would be advantageous in smaller or remote river systems where 'conventional' airborne TIR is too costly and traditional in-stream measurements risk missing local spatial variation. However, it is worth noting that these applications present situations where the thermal impacts of discrete temperature inputs may be unknown, may vary seasonally, and may have mixing

patterns that are difficult to discern. Therefore, simultaneous acquisition of in-stream temperature data is essential to validate the findings of sUAS-based TIR-based datasets.

4.2 Sources of bias and suggested methodological improvements

Although the drift observed within this study represents a considerable challenge to the derivation of diffuse river temperature heterogeneity from TIR imagery, results of the regression analysis and CCA indicate that the drift may have identifiable systematic elements (Fig 2B). Thus, it may be possible to take steps to improve the accuracy of TIR-derived temperatures. K_{in} was identified as the most important covariate governing long profile variability, presumably caused by the impact of radiative warming on the camera (and thus drift). Similarly, the relative strength of *TS* is likely due to the role of topographic shading from the mountainous Baddoch Burn terrain in controlling streamwise variability in the receipt of solar radiation by (and hence, radiative warming of) the camera. Elapsed time was also identified as an important covariate, in agreement with Mesas-Carrascosa et al. (2018). This variable integrates both time of day (comprising diurnal air temperature variation) and time passed during the survey (potentially corresponding to heat build-up due to energy dissipation from internal electronics). Thus, time can also be considered a proxy both for the external and internal heating of the TIR camera. This also explains the moderate importance of T_a as a covariate. Relative humidity was also found to be a strong covariate, presumably because overcast conditions which accompanied increased *RH* (particularly on 11 July) reduced radiative warming (and possibly aided sensible cooling) of the camera. These findings indicate that it may be feasible to minimise thermal drift (to a limited extent) by planning surveys to coincide with overcast conditions which would limit external (radiative) camera warming. However, given that TIR survey flights should generally be conducted on warm/sunny days and during low flows to exploit the increased thermal difference from cool advective inputs and radiative warming of the channel (eg. Dugdale, 2016), this may not be a practical solution. In our investigation, we conducted flights throughout the day with a view to characterising temporal change in the Baddoch Burn's longitudinal temperature profile, and we acknowledge that this practise may have increased drift in comparison to if we had consistently conducted flights later in the day (coinciding with reduced solar radiation). However, although these findings might also be construed to suggest that conducting surveys during night-time will reduce radiative warming, systematic testing of similar miniaturised drone-based cameras during night-time suggests that this practise does not eliminate drift (E. Baker, personal communication), presumably as other sources of interference (e.g. sensible and latent heat fluxes) are still present, something that we have also observed during ground-based testing at night. Indeed, our findings suggest that no single covariate is responsible for all of the temperature drift. While solar radiation was found to be the strongest covariate in general terms, surveys 4 and 6 exhibited relatively high levels of drift in spite of reduced solar radiation. On these occasions, it is likely that a combination of other covariates (eg. topographic shading and relative humidity, which were particularly pronounced during surveys 4 and 6 respectively) explain the majority of the drift.

While external flight characteristics and environmental metrics explained 66% of the long profile variability, the remaining 34% is unaccounted for. This remaining variability is presumably a combination of true diffuse river temperature heterogeneity and internal sensor warming due to power dissipation from camera circuitry (Olbrycht and Więcek 2015; Strąkowki 2017). Not only does this partially account for why drift is present in night-time flights, but also indicates that even through minimising all external sources of drift, it will still be difficult to separate true diffuse heterogeneity from drift caused by internal sensor warming. Although researchers have published a range of drift compensation methods, these are either experimental hardware-based techniques (eg. Olbrycht and Więcek 2015; Ribeiro-Gomes et al. 2017) or involve modelling or

additional image acquisition to remove inter-image bias and 'normalise' image sequences (eg. Abolt et al., 2018; Jensen et al. 2014; Mesas-Carrascosa et al. 2018), which, when applied over the spatial scales at which diffuse thermal heterogeneity occurs (10^2 – 10^4 m), may also have the unwanted effect of removing true longitudinal temperature variability present within the image series. We therefore advocate the development of new processing techniques specific to river environments that are capable of compensating for sUAS-based TIR drift while preserving true streamwise temperature variability. Two promising avenues of research include the use of image mosaics to quantify (and thus, remove) the inter-image bias as a function of the temperature difference between overlapping image segments (similar to the method of Abolt et al., 2018), or the use of statistical river temperature models with river network smoothers to 'detrend' the image data based on temperature records from loggers (e.g. Jackson et al. 2017). These techniques are the subject of ongoing research by the authors. The simultaneous acquisition of river temperature data using ground-based/handheld TIR cameras also holds potential for enhancing TIR data collection using drones. Indeed, recent research (eg. Bonar & Petre, 2015; Hare et al. 2015; Ganji et al., 2016) has demonstrated that such methods are both a cost-effective and relatively simple technique for acquiring spatially-explicit river temperature data. The collection of ground-based temperature data at the same time as sUAS imagery surveys may therefore prove useful for compensating for drift observed here.

5. Conclusions

While sUAS-based TIR can produce high resolution imagery that clearly delineates the extent and location of discrete advective thermal inputs to streams, our results do not currently support the use of certain popular miniaturised TIR camera solutions (such as those discussed in this article) to quantify true river temperature data without substantial correction using distributed kinetic temperature data (that may substantially increase resource requirements and thus reduce the overall value of TIR data). Both inter-image biases (temperature drift) and within-image biases (resulting from solar/skylight reflections in each image) generated substantial differences between radiant and kinetic temperatures in two different river systems. Statistical approaches to separate the drivers of long profile variability across flights demonstrate that temperature drift is partially the result of flight conditions and environmental variables, but more work remains to separate other (eg. internal) drivers of errors. sUAS-based TIR represents a promising approach for collecting data at spatial scales situated between 'conventional' remote sensing approaches and point measurements. However, this potential cannot be truly realised without further developments to correct for the biases observed here. Without such development, the primary value of these data is for identifying and delineating discrete thermal inputs where true temperatures are less important. We therefore call for enhanced clarity and reporting of (potentially negative) results by those using drone-based TIR cameras in the hydrological sciences in order to develop thorough recommendations for the 'best-practise' collection of water temperature data using TIR. Nevetheless, ongoing technological advancements at the interface of sensor technologies and sUAS platforms will no doubt yield future improvement in the extraction of quantitative temperature data for future research endeavours.

Acknowledgements

This project has received funding from the European Union's Horizon 2020 research and innovation programme under the Marie Skłodowska-Curie Grant Agreement No. 702468. IAM's contribution forms part of Marine Scotland Service Level Agreement FW02G. We would like to thank Stephen McLaren, Denise Stirling, Pauline Proudlock and Ross Glover of Marine Scotland for help with data collection in the Baddoch

Burn. We also thank the Invercauld Estate for permission to conduct the sUAS surveys. Syracuse data collection was made possible through funding from the Syracuse Center of Excellence, piloting by Ian Joyce (Syracuse University Center for Advanced Systems and Engineering), and several volunteer visual observers that assisted with each flight. This article benefited from the constructive comments of two anonymous reviewers.

References

Abolt, C., Caldwell, T., Wolaver, B., & Pai, H. (2018). Unmanned aerial vehicle-based monitoring of groundwater inputs to surface waters using an economical thermal infrared camera. *Optical Engineering*, 57, 5, 053113, DOI: 10.1117/1.OE.57.5.053113

Adobe (2017). *Photoshop CC 2017*. San Jose, California, USA: Adobe Systems Inc

Agisoft (2017). *Photoscan Professional*. St. Petersburg, Russia: Agisoft LLC

Arismendi, I., Johnson, S.L., Dunham, J.B., Haggerty, R., & Hockman-Wert, D. (2012). The paradox of cooling streams in a warming world: Regional climate trends do not parallel variable local trends in stream temperature in the Pacific continental United States. *Geophysical Research Letters, 39*, DOI: 10.1029/2012GL051448

Arnell, N.W., & Gosling, S.N. (2013). The impacts of climate change on river flow regimes at the global scale. *Journal of Hydrology, 486*, 351-364

Bonar, S.A., & Petre, S.J. (2015). Ground-Based Thermal Imaging of Stream Surface Temperatures: Technique and Evaluation. *North American Journal of Fisheries Management*, 35, 1209-1218

Brewitt, K.S., & Danner, E.M. (2014). Spatio-temporal temperature variation influences juvenile steelhead (Oncorhynchus mykiss) use of thermal refuges. *Ecosphere, 5*, 1-26

Briggs, M.A., Dawson, C.B., Holmquist-Johnson, C.L., Williams, K.H., & Lane, J.W. 2018. Efficient hydrogeological characterization of remote stream corridors using drones. *Hydrological Processes*, DOI: 10.1002/hyp.13332

Caissie, D. (2006). The thermal regime of rivers: a review. *Freshwater Biology, 51*, 1389-1406

Chen, D., Hu, M., Guo, Y., & Dahlgren, R.A. (2016). Changes in river water temperature between 1980 and 2012 in Yongan watershed, eastern China: Magnitude, drivers and models. *Journal of Hydrology, 533*, 191-199

Daigle, A., Jeong, D.I., & Lapointe, M.F. (2015). Climate change and resilience of tributary thermal refugia for salmonids in eastern Canadian rivers. *Hydrological Sciences Journal, 60*, 1044-1063

Dugdale, S.J. (2016). A practitioner's guide to thermal infrared remote sensing of rivers and streams: recent advances, precautions and considerations. *Wiley Interdisciplinary Reviews: Water, 3*, 251-268

Dugdale, S.J., Bergeron, N.E., & St-Hilaire, A. (2013). Temporal variability of thermal refuges and water temperature patterns in an Atlantic salmon river. *Remote Sensing of Environment, 136*, 358-373

Dugdale, S.J., Bergeron, N.E., & St-Hilaire, A. (2015). Spatial distribution of thermal refuges analysed in relation to riverscape hydromorphology using airborne thermal infrared imagery. *Remote Sensing of Environment, 160*, 43-55

Ebersole, J.L., Wigington Jr, P.J., Leibowitz, S.G., Comeleo, R.L., & Sickle, J.V. (2015). Predicting the occurrence of cold-water patches at intermittent and ephemeral tributary confluences with warm rivers. *Freshwater Science, 34*, 111-124

Eschbach, D., Piasny, G., Schmitt, L., Pfister, L., Grussenmeyer, P., Koehl, M., Skupinski, G., & Serradj, A. (2017). Thermal-infrared remote sensing of surface water–groundwater exchanges in a restored anastomosing channel (Upper Rhine River, France). *Hydrological Processes, 31*, 1113-1124

ESRI (2014). *ArcMap 10.3*. Redlands, CA: Environmental Systems Resource Institute

Fitch, K., Kelleher, C., Caldwell, S., & Joyce, I. (2018). Airborne thermal infrared videography of stream temperature anomalies from a small unoccupied aerial system. *Hydrological Processes*, 32, 2616-2619

FLIR (2018). *FLIR Tools 6.4*. Wilsonville, Oregon, USA: FLIR Systems Inc

Frechette, D.M., Dugdale, S.J., Dodson, J.J., & Bergeron, N.E. (2018). Understanding summertime thermal refuge use by adult Atlantic salmon using remote sensing, river temperature monitoring, and acoustic telemetry. *Canadian Journal of Fisheries and Aquatic Sciences*. DOI: 10.1139/cjfas-2017-0422

Fullerton, A.H., Torgersen, C.E., Lawler, J.J., Faux, R.N., Steel, E.A., Beechie, T.J., Ebersole, J.L., & Leibowitz, S.G. (2015). Rethinking the longitudinal stream temperature paradigm: region-wide comparison of thermal infrared imagery reveals unexpected complexity of river temperatures. *Hydrological Processes, 29*, 4719-4737

Fullerton, A.H., Torgersen, C.E., Lawler, J.J., Steel, E.A., Ebersole, J.L., & Lee, S.Y. (2018). Longitudinal thermal heterogeneity in rivers and refugia for coldwater species: effects of scale and climate change. *Aquatic Sciences, 80*, 3

Gangi, L., Hannah, D. & Weiler, M. (2016). Microthermal variability in a Welsh upland stream. In: Gilvear, D., Greenwood, M., Thoms, M. & Wood, P (Eds.). *River Science: Research and Management for the 21st Century*. Chichester, Wiley-Blackwell, p. 279-294

Garner, G., Hannah, D.M., & Watts, G. (2017a). Climate change and water in the UK: Recent scientific evidence for past and future change. *Progress in Physical Geography, 41*, 154-170

Garner, G., Malcolm, I.A., Sadler, J.P., & Hannah, D.M. (2017b). The role of riparian vegetation density, channel orientation and water velocity in determining river temperature dynamics. *Journal of Hydrology, 553*

George, S.D., Baldigo, B.P., Smith, M.J., McKeown, D.M., & Faulring, J.W. (2016). Variations in water temperature and implications for trout populations in the Upper Schoharie Creek and West Kill, New York, USA. *Journal of Freshwater Ecology, 31*, 93-108

Goldman, D.B., 2010. Vignette and exposure calibration and compensation. *IEEE Trans. Pattern Anal. Mach. Intell*. 32, 2276–2288

Handcock, R.N., Gillespie, A.R., Cherkauer, K.A., Kay, J.E., Burges, S.J., & Kampf, S.K. (2006). Accuracy and uncertainty of thermal-infrared remote sensing of stream temperatures at multiple spatial scales. *Remote Sensing of Environment, 100*, 427-440

Handcock, R.N., Torgersen, C.E., Cherkauer, K.A., Gillespie, A.R., Tockner, K., Faux, R.N., & Tan, J. (2012). Thermal Infrared Remote Sensing of Water Temperature in Riverine Landscapes. In: Carbonneau P.E. and Piégay, H, *Fluvial Remote Sensing for Science and Management* (pp. 85-113). Chichester, UK: John Wiley & Sons

Hannah, D.M., & Garner, G. (2015). River water temperature in the United Kingdom: Changes over the 20th century and possible changes over the 21st century. *Progress in Physical Geography, 39*, 68-92

Hare, D.K., Briggs, M.A., Rosenberry, D.O., Boutt, D.F., & Lane, J.W. (2015). A comparison of thermal infrared to fiber-optic distributed temperature sensing for evaluation of groundwater discharge to surface water. *Journal of Hydrology*, 530, 153-166

Harvey, P. (2018). ExifTool 10.80. Available at: https://www.sno.phy.queensu.ca/~phil/exiftool/ (accessed 2018-07-05)

Isaak, D.J., Young, M.K., Nagel, D.E., Horan, D.L., & Groce, M.C. (2015). The cold-water climate shield: delineating refugia for preserving salmonid fishes through the 21st century. *Global Change Biology, 21*, 2540-2553

Jackson, F.L., Hannah, D.M., Fryer, R.J., Millar, C.P., & Malcolm, I.A. (2017). Development of spatial regression models for predicting summer river temperatures from landscape characteristics: Implications for land and fisheries management. *Hydrological Processes, 31*, 1225-1238

Jensen, A.M., McKee, M., & Chen, Y. (2013). *Calibrating thermal imagery from an unmanned aerial system - AggieAir.* Proceedings of the IEEE International Geoscience and Remote Sensing Symposium (IGARSS) 2013, 21-26 July. Melbourne, Australia: IEEE International, pp. 542-545

Jensen, A.M., Neilson, B.T., McKee, M., & YangQuan, C. (2012). *Thermal remote sensing with an autonomous unmanned aerial remote sensing platform for surface stream temperatures*. Proceedings of the IEEE Geoscience and Remote Sensing Symposium (IGARSS) 2012*,* 22-27 July, Munich, Germany: IEEE International, pp. 5049-5052

Jensen, A.M., McKee, M., Chen, Y. (2014). *Procedures for processing thermal images using low-cost microbolometer cameras for small unmanned aerial systems*. Proceedings of the 2014 IEEE Geoscience and Remote Sensing Symposium 2014, 13–18 July, Quebec City, QC, Canada: IEEE International, pp. 2629–2632

Jones, J.A., Creed, I.F., Hatcher, K.L., Warren, R.J., Adams, M.B., Benson, M.H., Boose, E., Brown, W.A., Campbell, J.L., Covich, A., Clow, D.W., Dahm, C.N., Elder, K., Ford, C.R., Grimm, N.B., Henshaw, D.L., Larson, K.L., Miles, E.S., Miles, K.M., Sebestyen, S.D., Spargo, A.T., Stone, A.B., Vose, J.M., & Williams, M.W. (2012). Ecosystem Processes and Human Influences Regulate Streamflow Response to Climate Change at Long-Term Ecological Research Sites. *BioScience, 62*, 390-404

Kelcey, J., Lucieer, A., 2012. Sensor correction of a 6-band multispectral imaging sensor for UAV remote sensing. *Remote Sensing*. 4, 1462–1493

Kim, M., Park, J.Y., Kopilevich, Y., Tuell, G., & Philpot, W. (2013). Correction for reflected sky radiance in low-altitude coastal hyperspectral images. *Applied Optics, 52*, 7732-7744

Kraaijenbrink, P.D.A., Shea, J.M., Litt, M., Steiner, JF, Treichler, D, Koch, I & Immerzeel, W.W. (2018). Mapping Surface Temperatures on a Debris-Covered Glacier With an Unmanned Aerial Vehicle. *Front. Earth Sci. 6.* DOI: 10.3389/feart.2018.00064

Kurylyk, B.L., MacQuarrie, K.T.B., Caissie, D., & McKenzie, J.M. (2015a). Shallow groundwater thermal sensitivity to climate change and land cover disturbances: derivation of analytical expressions and implications for stream temperature modeling. *Hydrol. Earth Syst. Sci., 19*, 2469-2489

Kurylyk, B.L., MacQuarrie, K.T.B., Linnansaari, T., Cunjak, R.A., & Curry, R.A. (2015b). Preserving, augmenting, and creating cold-water thermal refugia in rivers: concepts derived from research on the Miramichi River, New Brunswick (Canada). *Ecohydrology, 8*, 1095-1108

Lee, E., Yoon, H., Hyun, S.P., Burnett, W.C., Koh, D.-C., Ha, K., Kim, D.-j., Kim, Y., & Kang, K.-m. (2016). Unmanned aerial vehicles (UAVs)-based thermal infrared (TIR) mapping, a novel approach to assess groundwater discharge into the coastal zone. *Limnology and Oceanography: Methods, 14*, 725-735

MathWorks (2016). *MATLAB R2016a*. Natick, MA, USA: The MathWorks

Mesas-Carrascosa, F.-J., Pérez-Porras, F., Meroño de Larriva, J., Mena Frau, C., Agüera-Vega, F., Carvajal-Ramírez, F., Martínez-Carricondo, P., & García-Ferrer, A. (2018). Drift Correction of Lightweight Microbolometer Thermal Sensors On-Board Unmanned Aerial Vehicles. *Remote Sensing, 10*, 615

Miara, A., Pienkos, P.T., Bazilian, M., Davis, R., & Macknick, J. (2014). Planning for Algal Systems: An Energy-Water-Food Nexus Perspective. *Industrial Biotechnology, 10*, 202-211

Olbrycht, R., & Więcek, B. (2015). New approach to thermal drift correction in microbolometer thermal cameras. *Quantitative InfraRed Thermography Journal, 12*, 184-195

Olbrycht, R., Więcek, B., & De Mey, G. (2012). Thermal drift compensation method for microbolometer thermal cameras. *Applied Optics, 51*, 1788-1794

Rautio, A., Kivimäki, A.L., Korkka-Niemi, K., Nygård, M., Salonen, V.P., Lahti, K., & Vahtera, H. (2015). Vulnerability of groundwater resources to interaction with river water in a boreal catchment. *Hydrol. Earth Syst. Sci., 19*, 3015-3032

Ribeiro-Gomes, K., Hernández-López, D., Ortega, J.F., Ballesteros, R., Poblete, T., & Moreno, M.A. (2017). Uncooled Thermal Camera Calibration and Optimization of the Photogrammetry Process for UAV Applications in Agriculture. *Sensors, 17*, 2173

Steel, E.A., Beechie, T.J., Torgersen, C.E., & Fullerton, A.H. (2017). Envisioning, Quantifying, and Managing Thermal Regimes on River Networks. *BioScience, 67*, 506-522

Strąkowki, R. (2017). *Analysis of temperature drift in bolometric thermal imaging cameras.* PhD thesis, Lodz University of Technology, Institute of Electronics.

Tan, J., & Cherkauer, K.A. (2013). Assessing stream temperature variation in the Pacific Northwest using airborne thermal infrared remote sensing. *Journal of Environmental Management, 115*, 206-216

Taylor, R.G., Scanlon, B., Döll, P., Rodell, M., van Beek, R., Wada, Y., Longuevergne, L., Leblanc, M., Famiglietti, J.S., Edmunds, M., Konikow, L., Green, T.R., Chen, J., Taniguchi, M., Bierkens, M.F.P., MacDonald, A., Fan, Y., Maxwell, R.M., Yechieli, Y., Gurdak, J.J., Allen, D.M., Shamsudduha, M., Hiscock, K., Yeh, P.J.F., Holman, I., & Treidel, H. (2012). Ground water and climate change. *Nature Climate Change, 3*, 322

Tonolla, D., Wolter, C., Ruhtz, T., & Tockner, K. (2012). Linking fish assemblages and spatiotemporal thermal heterogeneity in a river-floodplain landscape using high-resolution airborne thermal infrared remote sensing and in-situ measurements. *Remote Sensing of Environment, 125*, 134-146

Torgersen, C.E., Faux, R.N., McIntosh, B.A., Poage, N.J., & Norton, D.J. (2001). Airborne thermal remote sensing for water temperature assessment in rivers and streams. *Remote Sensing of Environment, 76*, 386-398

Wawrzyniak, V., Piégay, H., Allemand, P., Vaudor, L., Goma, R., & Grandjean, P. (2016). Effects of geomorphology and groundwater level on the spatio-temporal variability of riverine cold water patches assessed using thermal infrared (TIR) remote sensing. *Remote Sensing of Environment, 175*, 337-348

Wawrzyniak, V., Piégay, H., Allemand, P., Vaudor, L., & Grandjean, P. (2013). Prediction of water temperature heterogeneity of braided rivers using very high resolution thermal infrared (TIR) images. *International Journal of Remote Sensing, 34*, 4812-4831

Webb, B.W., Hannah, D.M., Moore, R.D., Brown, L.E., & Nobilis, F. (2008). Recent advances in stream and river temperature research. *Hydrological Processes, 22*, 902-918

Wolf, A., Pezoa, J.E., & Figueroa, M. (2016). Modeling and Compensating Temperature-Dependent Non-Uniformity Noise in IR Microbolometer Cameras. *Sensors, 16*, 1121

Tables

Table 1. Characteristics of sUAS thermal imaging surveys of Baddoch Burn, Scotland

Survey no.	No. images	Date/time	Duration (MM:SS)	TIR camera yaw (°)	Altitude AGL (m)	Air temperature (°C)	Relative humidity (%)	Incoming shortwave radiation (W m^2)	Net radiation (W m^2)
1	239	2017-05-03 13:08	03:58	11.4	106.2	14.8	29.7	821.0	629.7
2	242	2017-05-03 14:38	04:02	11.7	106.3	14.2	28.2	522.9	376.3
3	241	2017-05-03 16:13	04:02	11.2	106.3	13.7	28.2	424.2	282.9
4	219	2017-05-03 17:29	03:38	12.1	105.8	12.4	25.8	94.2	-10.4
5	216	2017-07-11 11:46	03:36	11.1	100.0	12.0	69.5	334.3	251.8
6	209	2017-07-11 13:08	03:34	9.9	100.0	10.6	78.5	205.3	58.1
7	212	2017-07-12 11:14	03:36	11.1	100.0	13.5	56.7	505.8	405.2
8	217	2017-07-12 11:31	03:38	11.0	100.0	13.6	53.8	562.0	455.2
9	220	2017-07-12 11:55	03:40	0.1	100.0	13.8	51.8	344.5	250.9
10	192	2017-07-12 15:12	03:50	198.3	102.2	15.9	43.1	377.7	278.2

Table 2. Flight details for sUAS imagery acquisition in Syracuse, NY.

Survey no.	No. images	Date/time	TIR camera yaw (°)	Altitude AGL (m)	Air temperature (°C)	Relative humidity (%)
May (1)	20	2017-05-12 15:30	28	61	18.9	44
July (2)	14	2017-07-19 15:30	28	61	29.4	50

Table 3. Importance of covariates in stepwise multiple linear regression ($R^2 = 0.66$, $p < 0.001$) ranked from largest to smallest (ie. size of influence on temperature long profile). Covariates are incoming solar shortwave radiation (K_{in}), seconds elapsed since midnight (*time*), topographic shading (*TS*), relative humidity (*RH*), air temperature (T_a), sine of TIR camera yaw (sin_{cam}), altitude (*alt*) and sine of stream azimuth (sin_{azm})

Covariate	ΔBIC	*p*-value
K_{in}	289.91	<0.001
time	214.67	<0.001
TS	114.35	<0.01
RH	109.93	<0.001
T_a	43.89	<0.001
sin_{cam}	9.82	<0.001
alt	1.95	<0.001
sin_{azm}	0.49	<0.001

Figures

Figure 1. Maps of the study sites, including (a) Baddoch Burn, Scotland and (b) Onondaga Creek, Syracuse, NY

Figure 2. Drift-affected TIR image mosaics of Baddoch Burn showing (a) highest magnitude TIR drift observed over all flights (survey 3) and lowest magnitude TIR drift observed (survey 8). For more details on magnitude of drift, see Table S2.

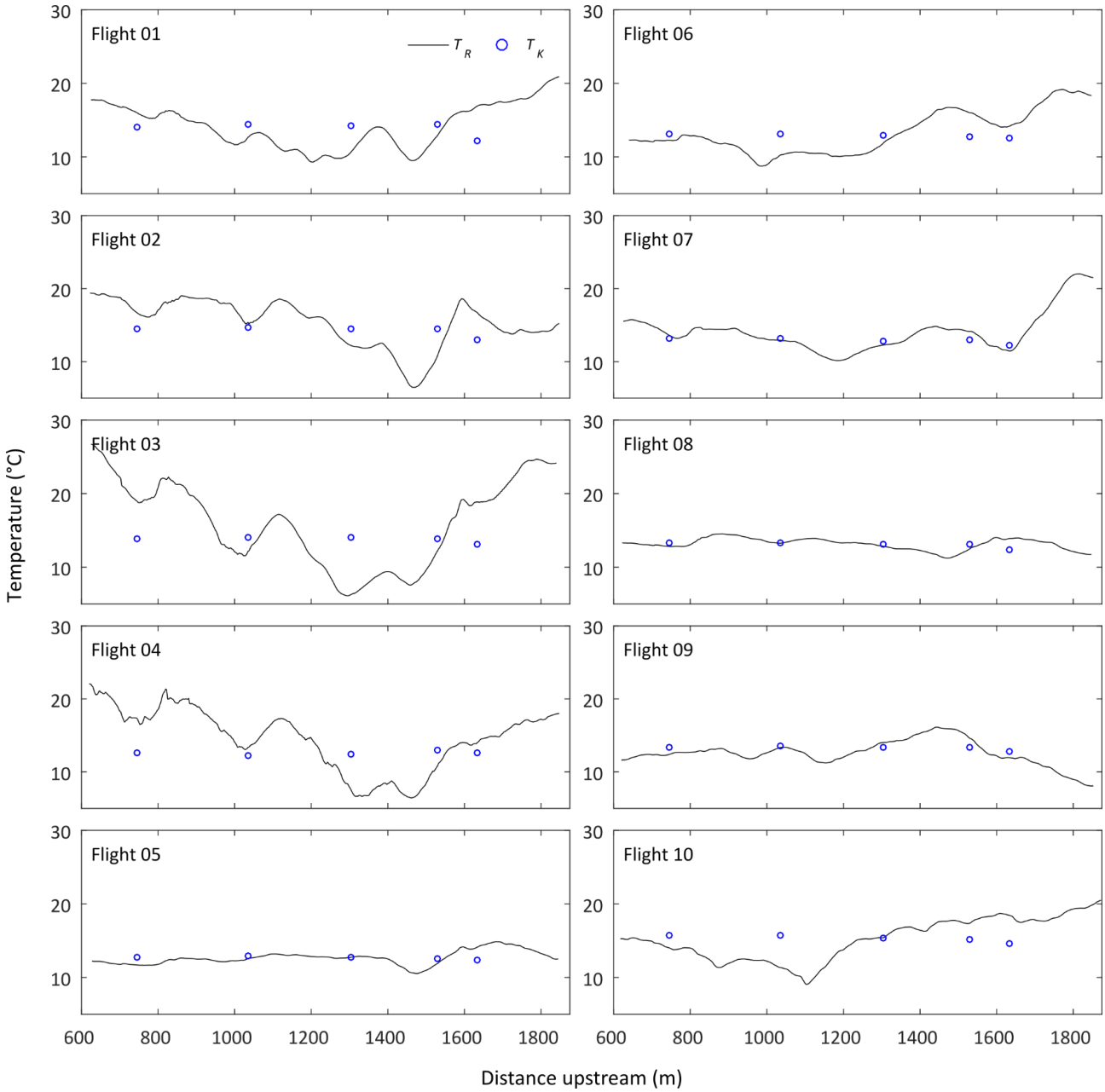

Figure 3. Temperature long profiles from 10 surveys of Baddoch Burn showing substantial temperature drift in TIR data (TR) in comparison to loggers (TK).

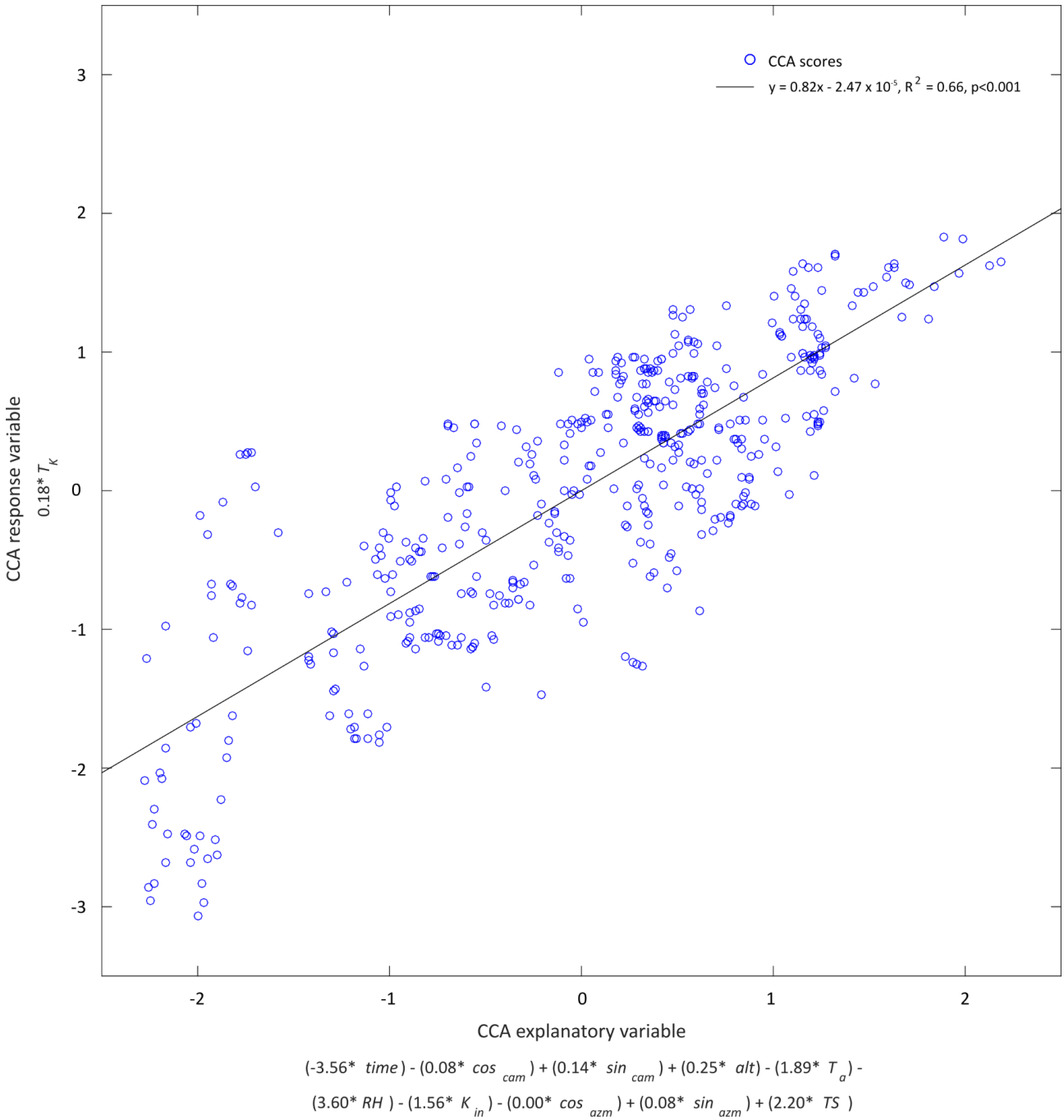

Figure 4. Canonical correlation analysis (CCA) showing positive relationship between flight / environmental metrics detailed in section 2.4 and temperature long profiles (including drift) derived from TIR data. Standardised CCA coefficients indicate relative influence of given covariate on TIR drift.

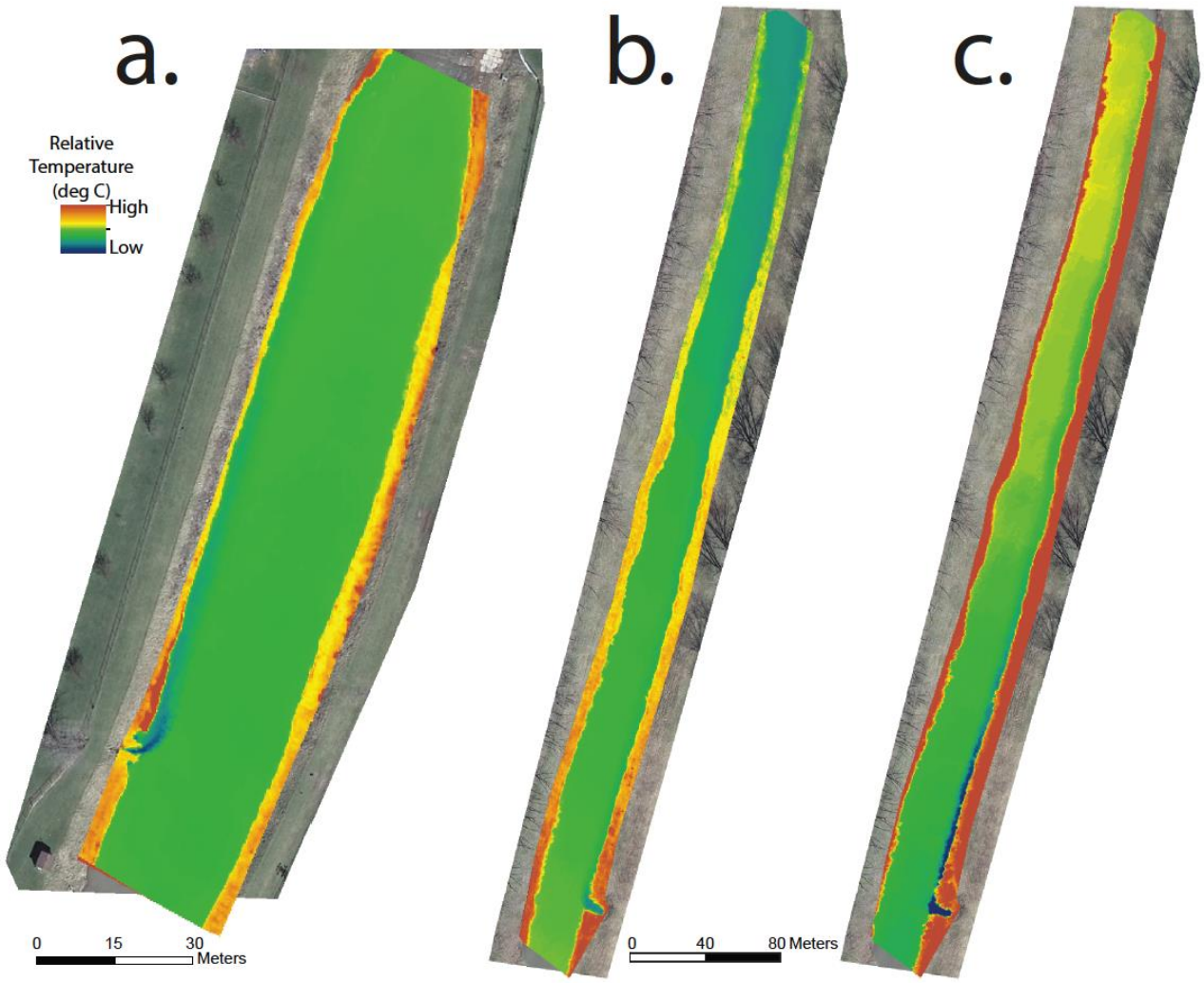

Figure 5. Post-processed TIR imagery along Onondaga Creek with relative stream temperatures for (a) the upstream spring during a May 2017 flight and the downstream active culvert during flights in (b) May and (c) July 2017.